Detailed microscopic study of the full ZipA : FtsZ interface

ARTICLE *in* PROTEINS STRUCTURE FUNCTION AND BIOINFORMATICS · JUNE 2006

Impact Factor: 2.63 · DOI: 10.1002/prot.20944 · Source: PubMed

3 AUTHORS, INCLUDING:

Irina Moreira
University of Coimbra
50 PUBLICATIONS **1,122** CITATIONS

SEE PROFILE

PROTEINS: Structure, Function, and Bioinformatics 63:811–821 (2006)

Detailed Microscopic Study of the Full ZipA:FtsZ Interface

I.S. Moreira, P.A. Fernandes, and M.J. Ramos*
Requimte/Departamento de Química, Faculdade de Ciências da Universidade do Porto, Porto, Portugal

ABSTRACT **Protein–protein interaction networks are very important for a wide range of biological processes. Crystallographic structures and mutational studies have generated a large number of information that allowed the discovery of energetically important determinants of specificity at intermolecular protein interfaces and the understanding of the structural and energetic characteristics of the binding hot spots. In this study we have used the improved MMPB/SA (molecular mechanics/Poisson-Boltzmann surface area) approach that combining molecular mechanics and continuum solvent permits to calculate the free energy differences upon alanine mutation. For a better understanding of the binding determinants of the complex formed between the FtsZ fragment and ZipA we extended the alanine scanning mutagenesis study to all interfacial residues of this complex. As a result, we present new mutations that allowed the discovery of residues for which the binding free energy differences upon alanine mutation are higher than 2.0 kcal/mol. We also observed the formation of a hydrophobic pocket with a high warm spot spatial complementarity between FtsZ and ZipA. Small molecules could be designed to bind to these amino acid residues hindering the binding of FtsZ to ZipA. Hence, these mutational data can be used to design new drugs to control more efficiently bacterial infections. Proteins 2006;63:811–821.** © 2006 Wiley-Liss, Inc.

Key words: microscopic study; ZipA:FtsZ interface; hot spots; alanine scanning mutagenesis; MM-PBSA; binding free energy

INTRODUCTION

Protein–protein interaction networks are very important for a wide range of biological processes. Crystallographic structures and mutational studies have generated a large amount of information that allowed the discovery of energetically important determinants of specificity at intermolecular protein interfaces. Therefore, a better understanding of the protein recognition process was achieved, which was important for drug and protein design (Structure Based Drug Design).[1–4]

Alanine scanning mutagenesis of protein–protein interfacial residues permits an exploration of the energetic contribution of individual side chains in protein binding. Interpretation of alanine scanning results allowed the definition of a hot spot as a region determinant for binding.[5] Therefore, a hot spot has been defined as a site where alanine mutations caused an increase in the binding free energy larger than 4.0 kcal/mol, even though lower values are used for statistical analyses.[6,7] The warm spots are those with binding free energy differences between 2.0 and 4.0 kcal/mol, and the null spots are the residues with binding free energy differences lower than 2.0 kcal/mol.[6]

There are no structural rules to predict the existence of a hot spot in an interface.[8] Because a hot spot has a significant energetic contribution to a protein–protein association, the residue identity, size, and charge, and the interactions it establishes with its neighbor residues are crucial. Even though the residues that interact with the hot spots are not always important for the protein–protein binding, nevertheless they may be expected to be conserved.[6] The interfacial binding hot spots are cooperative.[8]

Those hot spots of binding energy are usually enriched with tryptophan, tyrosine, and arginine,[9] and are not randomly spread along the protein–protein interfaces; they rather tend to be located near the center of the interface, and usually not exposed to the solvent. Solvent occlusion is a noteworthy but not sufficient condition to define a hot spot because other factors like being complementary to the van der Waals surface also contribute significantly.[7,9,10] However, a structure of an O-ring establishing a nonaqueous environment with a reduced effective dielectric constant for the hot spots in contrast with the high dielectric constant of water is often seen.[10]

A great effort has been invested in achieving a computational method that it is, at same time, detailed, fully atomistic, and with a high rate of success. In a recent article we have published a method capable of achieving an overall success rate of 80%, and a 100% success rate in residues for which alanine mutation causes an increase in the binding free energy higher than 4.0 kcal/mol (hot spots).[11] In this article, we show the advantage of a computational approach to systematically screen a receptor–ligand interface. This method was applied to a complex for which detailed knowledge is important for a better control of bacterial infection: the complex formed between the FtsZ fragment and ZipA[12] represented in Figure 1. FtsZ and ZipA are essential components of the septal ring machinery, which mediates cell division in *Escherichia coli*. In the cell, the protein assembles into a ring structure at the prospective division site early in the division cycle,

*Correspondence to: Maria João Ramos, Requimte/Departamento de Química, Faculdade de Ciências da Universidade do Porto, Rua do Campo Alegre 687, 4169-007 Porto, Portugal. E-mail: mjramos@fc.up.pt

Received 17 May 2005; Revised 30 September 2005; Accepted 26 October 2005

Published online 14 March 2006 in Wiley InterScience (www.interscience.wiley.com). DOI: 10.1002/prot.20944

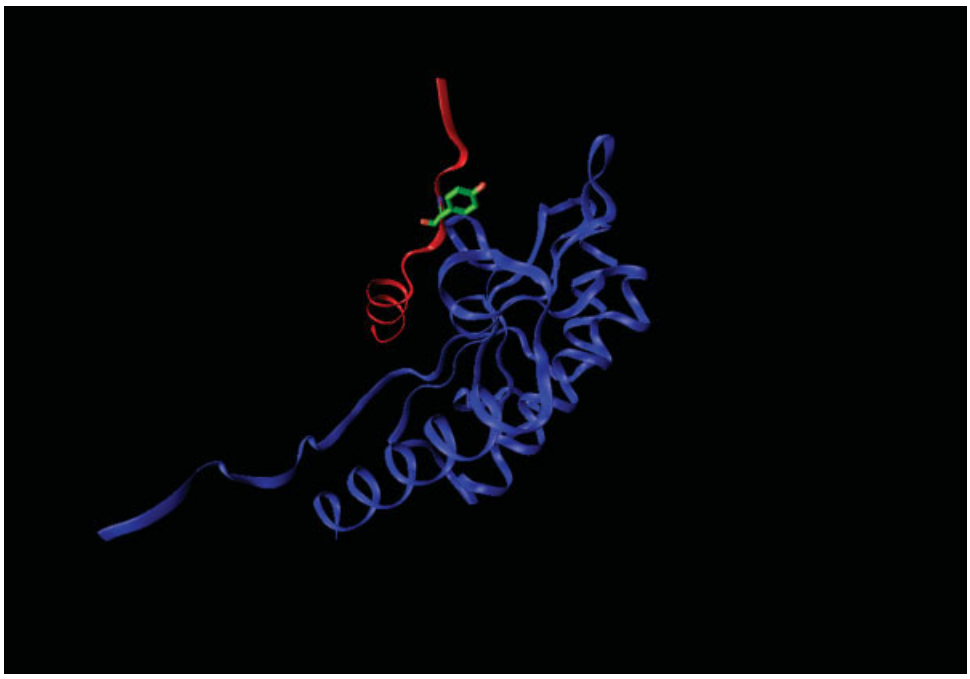

Fig. 1. The bacterial cell-division protein ZipA (in blue) and its interaction with an FtsZ fragment (in red) highlighting the Tyr371 residue by means of a licorice representation. [Color figure can be viewed in the online issue, which is available at www.interscience.wiley.com.]

and this marks the first recognized event in the assembly of the septal ring. FtsZ is a soluble, tubulin-like GTPase that forms a membrane-associated ring at the division site of bacterial cells constituting the most abundant of all bacterial cell division proteins. FtsZ is a crucial bacterial cell division protein that shows great similarity among bacterial species as well as homologs in almost all species of eubacteria and archaea. FtsZ recruits other cell division proteins, and it binds directly to an integral inner membrane protein in *E. coli*, the ZipA (Z interacting protein A). FtsZ recruits ZipA early in septation, while the Z-ring is still forming. This protein is an essential component of the division machinery, and is likely to be directly involved in the assembly and/or function of the FtsZ ring. The presence of ZipA is required to stabilize the Z-ring after it has formed, and to recruit other proteins to the septum.[13,14] The interaction between FtsZ and ZipA occurs through their carboxyl-terminal domains,[15] and it has been demonstrated that a single 17-amino acid peptide, corresponding to the FtsZ C-terminal residues 367–383, interacts with the C-terminal FtsZ binding domain of ZipA. Therefore, it constitutes the essential binding part of the protein. Once all the proteins have been localized, the Z-ring constricts, causing invagination of the membrane and bacterial cell division.

High numbers of antibiotics against bacterial infection are in use today, but the development of resistance by bacteria diminishes their effective power. The existing antibiotics have been subjected to extensive modifications to preserve the activity against their targets and overcome resistance.[16] However, their alteration is becoming increasingly hard, and therefore, new drugs against infectious bacterial diseases have to be developed. It is important to target unexplored indispensable proteins like the complex between FtsZ–ZipA to discovery new, noncrossresistant antibacterial agents.[17]

Thus, as bacterial infection is a worldwide health menace, the ZipA–Fts interaction is an outstanding target for antibacterial drug discovery in humans and in animals. Small-molecule inhibitors can be designed to bind to the residues of the complex between FtsZ with ZipA, hindering the complex formation, and therefore abolishing cell division.[16,17]

This study serves to provide a molecular view of the structural and energetic consequences of mutations. This computational approach leads to the interpretation of the mutations in terms of the contributions of the electrostatic and van der Waals interactions and those of solvation. Consequently, with a model that reproduces with high success rate the quantitative free energy differences obtained from experimental mutagenesis procedures, we are capable of anticipating the mutagenesis experimental results, thus guiding new experimental investigations.

Therefore, the main objective of this work is to obtain a deeper knowledge of an interface of protein–protein energetics, its critical points, subsequently allowing a control over the complex formation. This study also contributes to the generic knowledge of the protein interfaces, an important and fundamental theme in drug design.

MATERIALS AND METHODS

Model Setup

The starting crystallographic structure for the simulation, the complex formed between a cell division protein

ZipA and a cell division protein FtsZ, was taken from the RCSB Protein Data Bank with PDB entry 1f47[14] with a resolution of 1.95 Å, and a total of 1243 hydrogen atoms were added using the software Protonate from the Amber8 package.[18] The whole system comprised a total of 159 amino acids, 15 of which in the FtsZ protein (248 atoms) and 144 in the ZipA protein (2251 atoms). All residues were included in their physiological protonation states (charged Glu, Asp, Lys, and Arg, all other residues neutral). For the alanine scanning mutagenesis, we have followed a protocol already established to give a coherent agreement with the experimental results.[11] In the molecular simulations the solvent was modeled through a modified Generalized Born solvation model,[19] being the system in study (composed only by the complex) first minimized by 1000 steps of steepest decent followed by 1000 steps of conjugated gradient to release the bad contacts in the crystallographic structure. Afterward, a 4-ns molecular dynamics (MD) simulation in an infinite continuum medium with the dielectric properties of water using the Generalized born solvation model was performed starting from the minimized structure. All simulations were performed in an implicit dielectric solvent, and thus no counterions were added. All molecular mechanics simulations presented in this work were performed using the sander module, implemented in the Amber8[18] simulations package, with the *Cornell* force field.[20] Bond lengths involving hydrogens were constrained using the SHAKE algorithm,[21] and the equations of motion were integrated with a 2-fs time step being the nonbonded interactions truncated with a 16-Å cutoff. The temperature of the system was regulated by the Langevin thermostat.[22–24]

The MM_PBSA script implemented in Amber8[19] was used to calculate the binding free energies for the complex and for the alanine mutants. The MM_PBSA script[25] is used to do a postprocessing treatment of the complex by using the structure of the complex, and calculating the respective energies for the complex and all interacting monomers. To generate the structure of the mutant complex a simple truncation of the mutated side chain was made, replacing Cβ—Cγ with a hydrogen atom, and setting the Cβ—H bond direction to those of the former Cβ—Cγ. For the binding free energy calculations, 25 snapshots of the complexes were extracted every 20 ps for the last 500 ps of the run.

Alanine Scanning Mutagenesis

MM-PBSA, wherein only the initial and final states of the system are evaluated, is computationally less expensive than free energy perturbation methods, making it suitable for a greater variety of systems and problems, and representing a promising direction for evaluating binding affinities. This fully atomistic computational methodological approach consists in performing a MD simulation using a single trajectory of the wild-type structure, and subjecting it to a postprocessing treatment to generate the mutant structure without readjusting the surrounding protein environment to calculate $\Delta\Delta G_{\text{binding}}$. The use of the molecular mechanics AMBER force field and a continuum solvation approach with different internal dielectric constant values for different kinds of residues had led to the achievement of a computational alanine scanning mutagenesis methodological approach with a high success rate.[11]

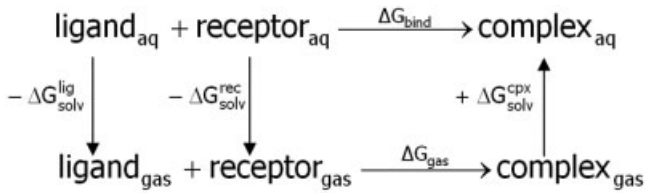

Scheme 1. Thermodynamic cycle used to calculate the complexation free energy.

The complexation free energy can be calculated using the thermodynamic cycle in Scheme 1, where $\Delta\Delta G_{\text{gas}}$ is the interaction free energy between the ligand and the receptor in the gas phase, and $\Delta G^{\text{lig}}_{\text{solv}}$, $\Delta G^{\text{rec}}_{\text{solv}}$, and $\Delta G^{\text{cpx}}_{\text{solv}}$ are the solvation free energies of the ligand, the receptor, and the complex, respectively. The binding free energy difference between the mutant and wild type complexes is defined as:

$$\Delta\Delta G_{\text{binding}} = \Delta G_{\text{binding-mutant}} - \Delta G_{\text{binding-wild type}} \quad (1)$$

The binding free energy of two molecules is the difference between the free energy of the complex and the respective monomers (the receptor and the ligand).

$$\Delta G_{\text{binding-molecule}} = G_{\text{complex}} - (G_{\text{receptor}} + G_{\text{ligand}}) \quad (2)$$

The free energy of the complex and respective monomers can be calculated by summing the internal energy (bond, angle, and dihedral), the electrostatic, and the van der Waals interactions, the free energy of polar solvation, the free energy of nonpolar solvation, and the entropic contribution for the molecule free energy:

$$G_{\text{molecule}} = E_{\text{internal}} + E_{\text{electrostatic}} + E_{\text{vdw}} + G_{\text{polar solvation}} + G_{\text{nonpolar solvation}} - \text{TS} \quad (3)$$

The first three terms were calculated using the *Cornell* force field[20] with no cutoff. The electrostatic solvation free energy was calculated by solving the Poisson-Boltzmann equation with the software Delphi v.4,[26,27] using the same methodology of previous works that has been shown in an earlier work to constitute a good compromise between accuracy and computing time.[28] In this continuum method, the protein is modeled as a dielectric continuum of low polarizability embedded in a dielectric medium of high polarizability.[26] It is assumed that the solvent is a homogeneous medium characterized by a single dielectric constant with a value usually near 80, which is taken to be equal to the bulk value for pure solvent. Separated by an abrupt interface, the solvent is in contact with the solute that is represented as a dielectric body whose shape is defined by atomic coordinates and radii. For the energy calculations three internal dielectric constant values, exclusively characteristic of the mutated amino acids were used: two for the nonpolar amino acids, three for the polar residues, and four for the charged amino acids.[11] The different internal dielectric constants mimicked the differ-

ent degree of relaxation of the interface when different types of amino acids are mutated for alanine.[11] We have treated the whole proteins with a single dielectric constant because we are calculating relative binding free energies, and in this case the differences between using different dielectric constants for each residue or using the same dielectric constant for the whole protein cancel when comparing the two binding free energies. The nonpolar contribution to solvation free energy due to van der Waals interactions between the solute and the solvent and cavity formation was modeled as a term that is dependent on the solvent-accessible surface area of the molecule. It was estimated using an empirical relation: $\Delta E_{\text{nonpolar}} = \sigma A + b$, where A is the solvent-accessible surface area that was estimated using the molsurf program, which is based on the idea primarily developed by Mike Connolly;[29] σ and b are empirical constants and the values used were 0.00542 kcal Å^{-2} mol^{-1} and 0.92 kcal mol^{-1}, respectively. The entropy term, obtained, as the sum of translational, rotational, and vibrational components, was not calculated because it was assumed, based in a previous work, that its contribution to $\Delta\Delta G_{\text{binding}}$ is negligible.[25]

The IC_{50} values of the experimental alanine mutagenesis data were used to calculate the experimental binding free energies using the following relationship: $\Delta G_{\text{binding}} = RT\ln IC_{50}$, where R is the ideal gas constant and T is the temperature in K.

Results

Alanine scanning mutagenesis of protein–protein interfacial residues is a very important process for rational drug design, and with a faster and reliable computational approach, it is possible to predict the binding affinities of the ligands. The improved MM-PB/SA is a fully atomistic method that combines molecular mechanics and continuum solvent as the basis for the methodology to probe protein–protein interactions by calculating free energies.[25,31–37]

To obtain reliable estimates of the relative binding energy of the 1f47 complex it was important to ensure that equilibration was achieved. In Figure 2a–c we have plotted the root-mean-square deviations (RMSD) from the X-ray crystal structure of the backbone atoms of the complex and the respective separate proteins, respectively. It can be observed that, after an initial period of 2000 ps of equilibration, the system has achieved equilibrium remaining very stable for the last 2000 ps of the computational simulation. The RMSD values are especially lower (1.8–2.0 Å) if we do consider only the receptor. The ligand is very small, consisting of only 15 amino acids, and its flexibility gives rise to higher RMSD values after 2 ns, due to a localized conformational transition corresponding to a slight opening of the end of the second turn of the FtsZ α-helix, which lies beyond the region where the binding determinants are located. Calculation of the RMSD restricted to the interface region shows a stable trend around 2 Å until the end of the simulation.

In Figure 3 we also plotted the total energy value (total energy = potential energy + kinetic energy) along the production dynamics simulation, which remains quite stable not presenting any large fluctuation.

Table I summarizes the results of the alanine scanning mutagenesis study of the protein–protein complex formed between the FtsZ fragment and the ZipA. The first nine interaction free energies in this table are energies for residues for which experimental values exist assessing the quality of the computational alanine scanning mutagenesis study.[14] It is important to highlight that a false warm spot was detected computationally, which can be explained by the fact that the corresponding residue (Tyr371) is not oriented to the interface (represented in Fig. 1). The computational method consists in using different internal dielectric constants to account for the different degree of relaxation at the interface when different types of amino acids are mutated for alanine. This way that residue, Tyr371, should not be subjected to this method that is calibrated to detect the correct binding free energy differences of interfacial residues with chain-sides located at the interface, and for which a internal dielectric value can be established based on the constituting amino acid residues of that specific protein region. Subsequently, in Table I, we present new mutations of the interfacial residues for a better understanding of the binding affinity between these two proteins.

To fully understand the binding free energy between FtsZ and ZipA, Table I and subsequently graphics present all the individual energy contributions to the relative binding free energy. Figure 4a–e present, respectively, the electrostatic energy $\Delta\Delta E_{\text{electrostatic}}$, the van der Waals energy $\Delta\Delta E_{\text{vdw}}$, the free energy of polar solvation $\Delta\Delta G_{\text{polar solvation}}$, the free energy of nonpolar solvation $\Delta\Delta G_{\text{nonpolar solvation}}$, and the binding free energy difference $\Delta\Delta G_{\text{binding}}$ between the mutant and wild-type complexes for all the mutated residues. The intermolecular electrostatic and the polar solvation free energy are important for protein–protein binding. These terms counteract each other, cancelling their effect, and subsequently we present in Figure 5 $\Delta\Delta G_{\text{polarsolvation}}$ as a function of $\Delta\Delta E_{\text{eletrostatic}}$. As a result of using a single trajectory protocol the internal energies cancel completely each other. From the Table I analysis, it can be observed that the nonpolar solvation contribution to the effective binding free energy difference is relatively small (less than 0.5 kcal/mol).

In the majority of the complexes, an analysis of the dominant interactions suggests that van der Waals interactions and hydrophobic effects provide a reasonable basis for understanding binding affinities.[38] From the analysis of Figure 4b it is perceived that the $\Delta\Delta E_{\text{vdw}}$ values are almost all positive, indicating that the van der Waals interaction is favorable to the complex binding, and that alanine mutation of the residues diminishes the vdW contacts at the interface. This fact is explained by the hydrophobic character of the interface. In this complex, the hydrophobic effects are dominant, and most of the direct interatomic contacts are hydrophobic contacts. From the experimental results,[12] we have the knowledge of the existence of three warm spots in the FtsZ peptide: Ile374, Phe377, and Leu378. These highly conserved residues are

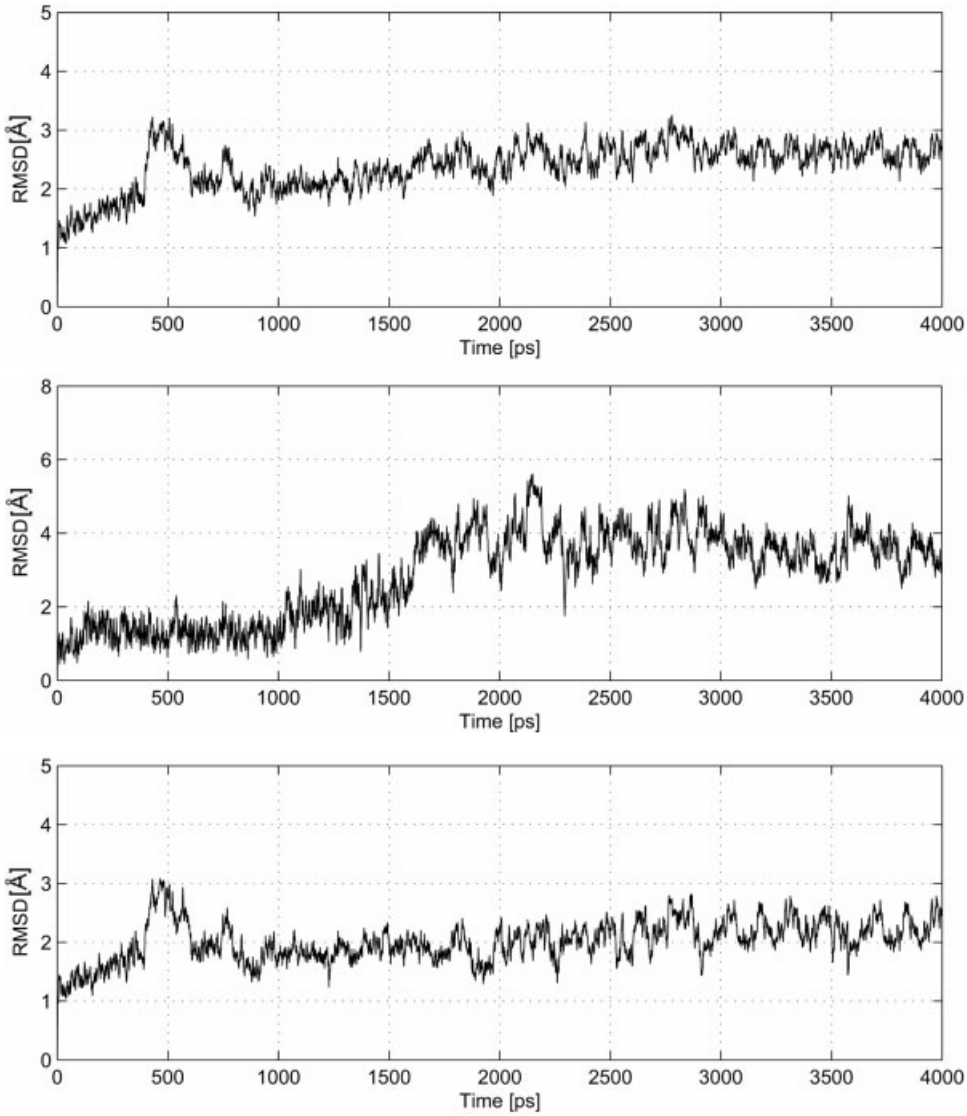

Fig. 2. RMSD plots for the protein backbone of the complex formed between the bacterial cell-division protein ZipA and the FtsZ fragment relative to its initial structure: (**a**) the complex, (**b**) the ligand, (**c**) the receptor.

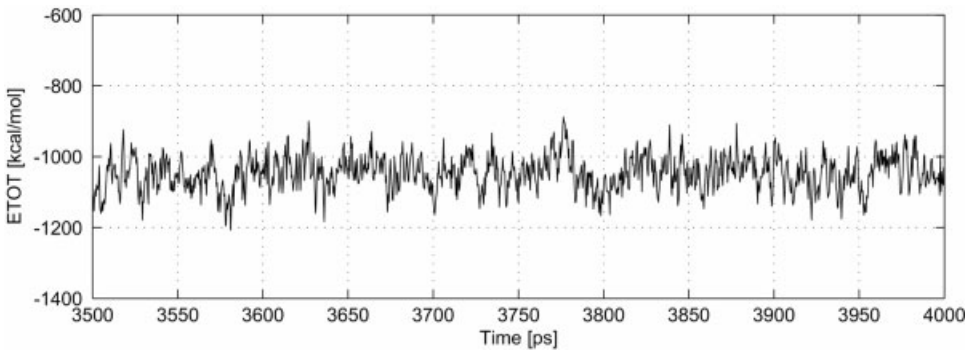

Fig. 3. Total energy values as a function of simulation time for the last 500 ps of the dynamics simulation for the complex formed between the bacterial cell-division protein ZipA and the FtsZ fragment.

TABLE I. Results of the Methodological Approach for Computational Alanine Screening Mutagenesis

Mutation		$\Delta\Delta E_{electrostatic}$	$\Delta\Delta E_{vdw}$	$\Delta\Delta G_{nonpolar\ solvation}$	$\Delta\Delta G_{polar\ solvation}$	$\Delta\Delta G_{binding}$	$\Delta\Delta G_{exp}$
FtsZ	Asp370Ala	−9.49	0.66	0.08	8.92	0.16 (0.90)	0.69
	Tyr371Ala	0.05	5.16	0.42	−2.42	3.20 (0.89)	0.86
	Leu372Ala	0.09	3.43	0.18	−2.67	1.01 (0.91)	0.92
	Asp373Ala	−17.19	0.40	0.00	16.15	−0.64 (0.90)	1.73
	Ile374Ala	0.32	5.46	0.26	−3.61	2.42 (0.78)	2.50
	Phe377Ala	−0.04	5.23	0.53	−3.23	2.48 (0.83)	2.44
	Leu378Ala	0.17	2.86	0.42	−0.61	2.73 (1.00)	2.29
	Arg379Ala	15.52	0.33	0.02	−14.77	1.08 (0.90)	0.00
	Lys380Ala	17.15	0.06	0.00	−16.18	1.01 (0.92)	0.00
ZipA	Val194Ala	0.74	0.87	0.08	0.06	1.73 (1.07)	NA
	Ile196Ala	0.51	1.80	0.09	−0.05	2.33 (1.07)	NA
	Asp225Ala	−1.45	0.02	0.00	1.82	0.38 (0.93)	NA
	Met226Ala	0.39	0.55	0.11	0.16	1.20 (1.02)	NA
	Ile228Ala	0.59	0.65	−0.01	−0.04	1.18 (1.04)	NA
	Asn247Ala	0.20	0.13	0.01	0.24	0.58 (0.93)	NA
	Met248Ala	0.93	1.10	−0.01	−2.40	−0.40 (0.97)	NA
	Val249Ala	−0.32	0.88	0.05	2.40	0.19 (1.07)	NA
	Lys250Ala	10.03	1.79	0.23	−9.99	2.06 (0.90)	NA
	Thr253Ala	0.31	0.38	0.03	0.08	0.79 (0.92)	NA
	Thr267Ala	0.23	0.64	−0.02	0.28	1.12 (1.02)	NA
	Ile268Ala	0.58	0.04	0.00	−0.15	0.46 (1.08)	NA
	Phe269Ala	0.57	2.93	0.09	−1.05	2.63 (1.06)	NA
	Met270Ala	0.56	0.03	0.00	0.28	0.86 (1.05)	NA
	Gln271Ala	0.33	0.46	0.04	−0.06	0.77 (0.91)	NA

The units of free energies and potential energies are kcal/mol.
NA—not available.

deeply or almost completely buried in hydrophobic pockets.

The FtsZ warm spots are oriented down into the cavity and their nonpolar side chains determine the shape and surface properties of the hydrophobic cavity.[14] Given the fact that for the three warm spots the magnitude of $\Delta\Delta G_{vdw}$ is higher (almost the double) than the magnitude of the sum of $\Delta\Delta G_{electrostatic}$ and $\Delta\Delta G_{polarsolvation}$, we conclude that the vdW (van der Waals) contacts are probably the driving force of the protein binding.

Considering the fact that there are often a significant number of charged and polar residues fully or partially buried in protein–protein interfaces, the specificity of association is greatly influenced by the presence of polar residues because electrostatic complementarity between the individual molecules further optimizes binding.[39,40] Although the overall structure of this complex interface is uncharged, being mainly hydrophobic, small but significant local charge–charge interactions do occur. By observation of Table I and Figure 4a and 4d it can be concluded that the $\Delta\Delta G_{electrostatic}$ and $\Delta\Delta G_{polar\ solvation}$ values for the polar residues are 10–15 kcal/mol higher than for the nonpolar amino acid. The high energy values are in agreement with the use of a dielectric constant of 4 to mimic the protein relaxation and reorganization as well as the electronic polarization that affects the charge–charge interactions.[11] During protein binding, the charged groups in the proteins desolvate as their environments change from aqueous to largely nonpolar solvent, causing huge electrostatic and polar solvation energy differences.[40] Nevertheless, if we only consider their sum we find that its value ranges between −1.0 and 1.0 kcal/mol.

Based on earlier results from alanine mutagenesis investigation obtained on numerous protein–protein interfacial residues,[41] it should be expected that functionally important residues on ZipA are those that are in direct contact with the key binding determinants of the FtsZ (Ile374, Phe377, and Leu378).[14] If we examine the binding free energy values in Table I and Figure 4e we can observe the achievement of three warm spots in protein ZipA: Ile196, Lys250, and Phe269. We have also noticed the importance of residue Val194 with an energy binding difference of 1.73 kcal/mol. Lys250 is a charged residue that interrupts the hydrophobic nature of the cavity[14] and has the side chain oriented to the interface and does not establish significant specific, short-range interactions with the neighboring residues. However, it is 4.72 Å apart from Asp373, indicating that probably it establishes a water-bridge ion pair with the carboxyl group from Asp373.

To evaluate in more detail the role of the amino acid residues present in the binding interface, we have also performed simultaneous alanine mutagenesis (alanine shaving), and the results are present in Table II. For the three warm spots (Ile374, Phe377, and Leu378) we have obtained a $\Delta\Delta G_{binding}$ value of 9.83 kcal/mol, accessing the importance of these residues for the protein binding. This $\Delta\Delta G_{binding}$ value is greater than the one predicted, assuming simple additivity of the effects of individual alanine mutation, stressing the cooperative effect of the binding hot spots. In contrast with the mutations within this

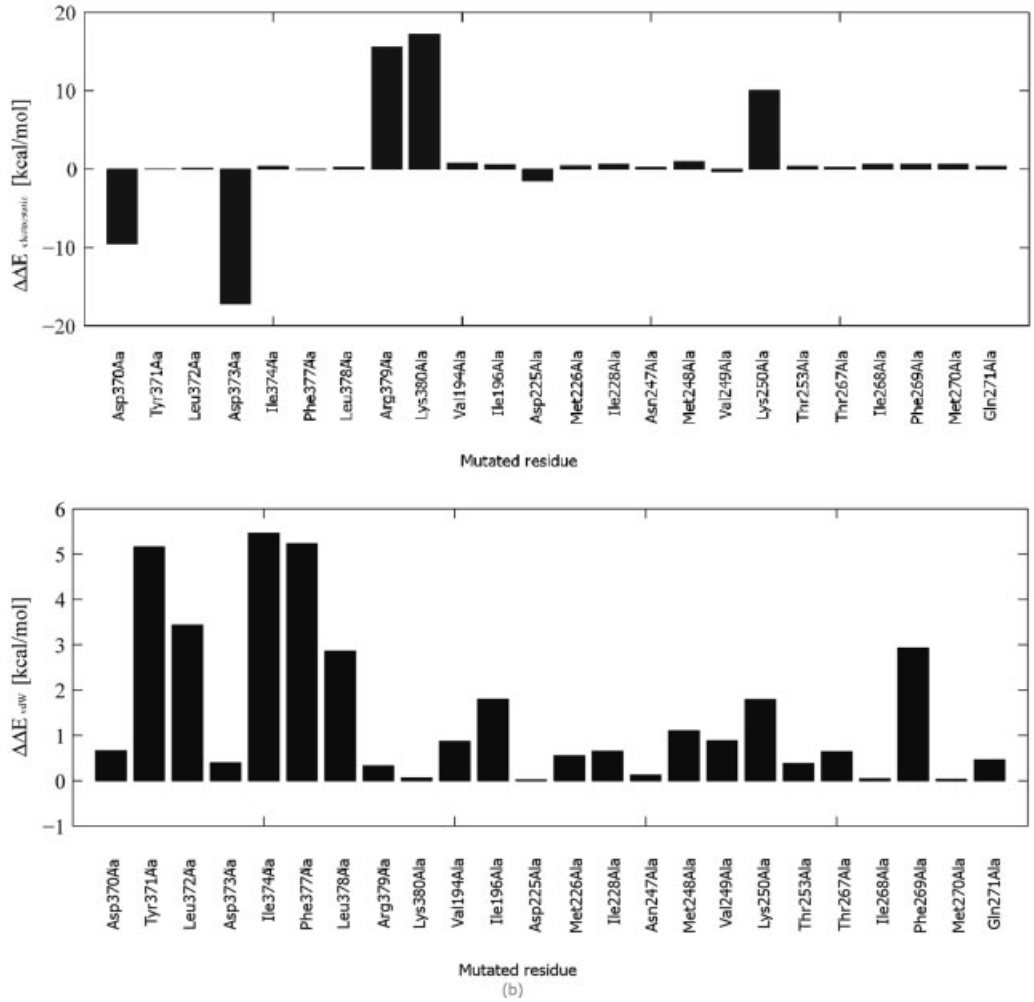

Fig. 4. (**a**) Electrostatic energy $\Delta\Delta E_{\text{electrostatic}}$, (**b**) van der Waals energy $\Delta\Delta E_{\text{vdw}}$, (**c**) free energy of polar solvation $\Delta\Delta G_{\text{polar solvation}}$, (**d**) free energy of nonpolar solvation $\Delta\Delta G_{\text{nonpolar solvation}}$, and (**e**) binding free energy difference $\Delta\Delta G_{\text{binding}}$ between the mutant and wild-type complexes for all the mutated residues.

cluster, the combinations made between the most important residues in the other binding partners (Val194, Ile196, and Phe269) were not cooperative. These results are consistent with an increase of the spatial separation between the residues that constitute this cluster. We also made alanine shaving of null spot clusters of this complex (Met248 and Val249; Asp370, Lys380, and Asp225), and we have not detected a cooperative positive effect. In fact, we have detected a decrease in the binding free energy in comparison with the individual contribution sum, showing an improvement of the binding affinity that further supports the notion that these residues do not have a significant contribution to the binding free energy.

Recalling that the interface is essentially hydrophobic, we are now in a position to justify the warm spot character of Ile196, Phe269, and the importance of Val194. From the analysis of Table I and Figure 4a–e, we emphasize yet again the vdW interaction importance as the dominant factor that leads to stable complex formation, because the binding free energies are in the same order as the vdW interactions energies. The importance of the hydrophobic pocket and the vdW interaction leads to the finding that steric complementarity should probably be the determinant factor to promote complex formation. The surfaces between FtsZ and ZipA are complementary, largely consisting of the side chain of each protein's nonpolar residues, with the nonpolar regions of both proteins juxtaposed. The warm spots of binding energy are located near the center of the interfaces and upon complexation, the two "warm-spot clusters" come into contact across the interfaces as it can be seen in Figure 6. As already established for other complexes,[10] in this one there is large complementarity both in shape and in the juxtaposition of hydrophobic amino acid residues. The warm spot of one face packs against the warm spot of its binding partner establishing a pocked region determinant for complex binding.

There are two independent binding determinants in this interface. A pair of warm-spot clusters, one in each protein, that exhibit notorious shape complementarity, and where pack one against the other can be observed. The warm spot character of this cluster can be explained structurally by its presence near the center of the contact

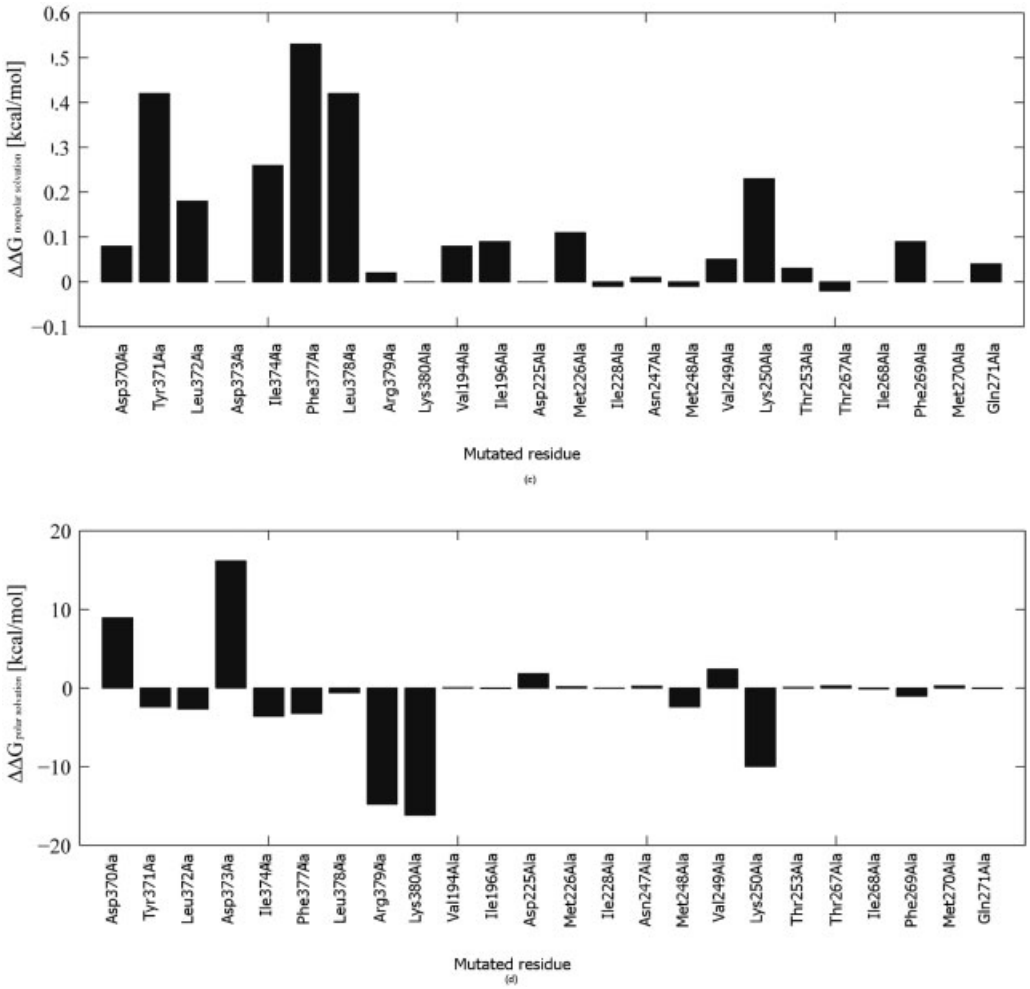

Figure 4. (Continued).

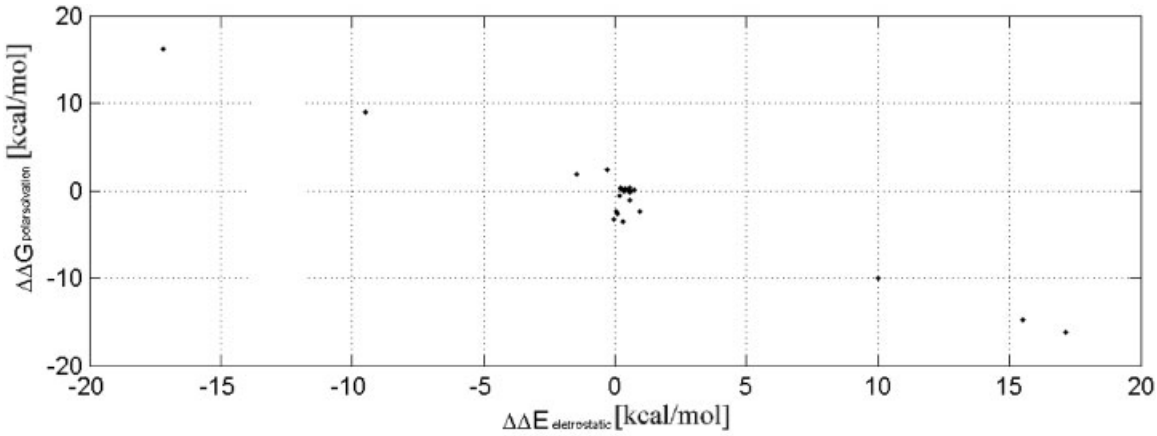

Fig. 5. Free energy of polar solvation $\Delta\Delta G_{\text{polarsolvation}}$ as a function of electrostatic energy difference $\Delta\Delta E_{\text{eletrostatic}}$ between the mutant and wild-type complexes for all the mutated residues.

interface. Alanine mutation of these residues diminishes the nonpolar surface area and the optimal vdW contacts at the interface that are essential to complex formation. Three residues constitute each of these clusters, namely Ile374, Phe377, and Leu378 in FtsZ and Val194, Ile196, and Phe269 in ZipA. Strictly speaking, Val194 is not a warm spot, as its $\Delta\Delta G_{\text{binding}}$ of 1.73 kcal/mol is below the 2 kcal/mol threshold, characteristic of a warm spot. This

TABLE II. Results of Alanine Showing

Mutation	$\Delta\Delta G_{calculated}$ [kcal/mol]	$\Sigma\Delta\Delta G_{calculated}$ [kcal/mol]	Cooperativity (kcal/mol)
Ile374Ala/Phe377Ala/Leu378Ala	9.83	7.63	2.20
Val194Ala/Ile196Ala/Phe269Ala	5.24	5.69	−0.45
Met248Ala/Val249Ala	−0.69	−0.21	−0.48
Asp370/Lys380Ala/Asp225Ala	0.42	1.55	−1.13

The units of free energies are kcal/mol.

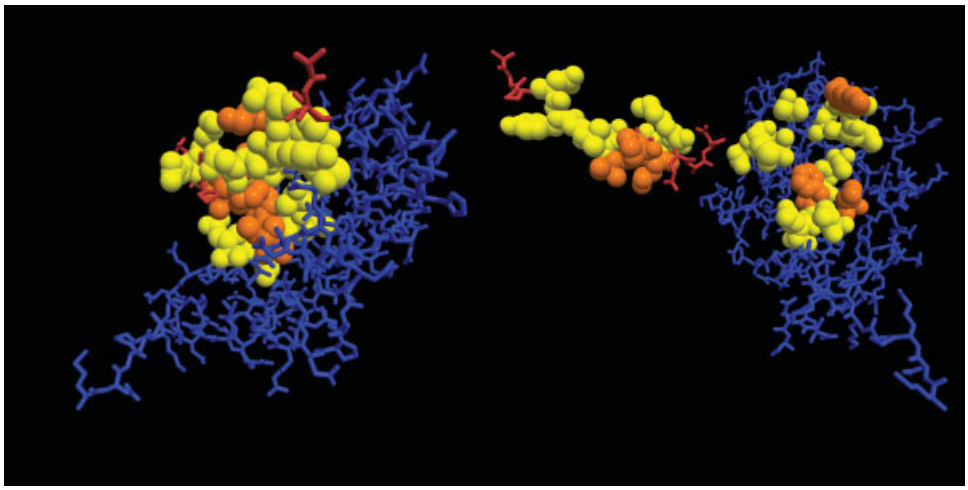

Fig. 6. Complex formed between the bacterial cell-division protein ZipA and the FtsZ fragment highlighting the mutated residues in the two binding interfaces by means of a ball-and-stick representation. Yellow represents the null spots (relative binding energy <2.0 kcal/mol) and orange the warm-spots (relative binding energy between 2.0 and 4.0 kcal/mol).

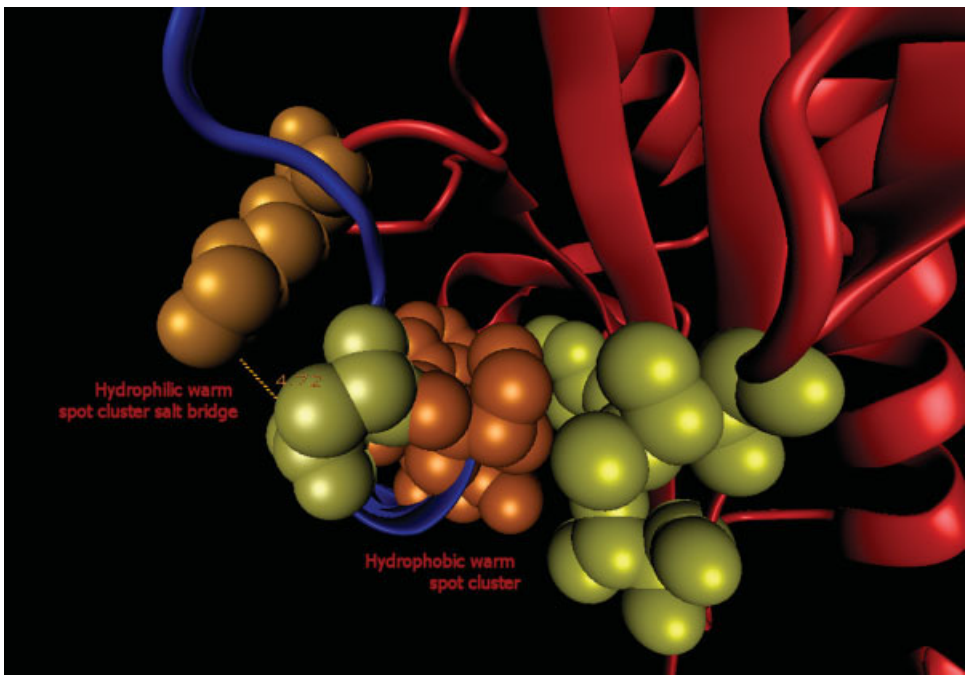

Fig. 7. Complex formed between the bacterial cell-division protein ZipA (red) and the FtsZ fragment (blue) highlighting the warm spot residues in the two binding interfaces by means of a ball-and-stick representation.

binding determinant is hydrophobic in nature, and the burial of the complementary hydrophobic surfaces upon binding favors the bound state.

The other binding determinant is constituted by the *quasi* warm-spot Asp373 ($\Delta\Delta G_{exp}$ of 1.73 kcal/mol) in FtsZ and the warm-spot Lys250 in ZipA. In this case, the binding determinant is hydrophilic, and is due to a salt bridge between the two charged residues. The salt bridge is somewhat shielded by the solvent, due to significant residue exposure (distance of 4.72 Å between the carboxylate oxygen of Asp373 and the amine nitrogen of Lys250), which renders the moderate warm spot nature for this structure. Figure 7 illustrates the discussed structures.

In previous reports the existence of an O-ring structure that leads to the exclusion of bulk solvent from the interacting residues by the surrounding of the hot spot by a set of contacts that are energetically unimportant has been proposed.[10] In this complex this kind of formation had not been observed, which can be explained by the reduced size of this interface (the ligand has only 15 amino acids) and the existence of the hydrophobic pocket. We think that the solvent occlusion can be achieved in two different ways: the formation of an O-ring if the protein has a planar, large interface that allows for such a macromolecular structure, or alternatively, when the interface is too small, with the formation of a hydrophobic pocket. This hydrophobic pocket should be constituted by nonpolar amino acids with high $\Delta\Delta G_{binding}$ values, showing complementarity between both proteins in the complex, and allowing for the burying of the interacting residues.

CONCLUSION

Alanine scanning mutagenesis of protein–protein interfacial residues is a very important process for rational drug design. In this study we have used the improved MMPB/SA approach that combining molecular mechanics and continuum solvent permits to calculate the free energy differences upon alanine mutation.

For a better understanding of the binding determinants of the complex formed between the FtsZ and ZipA proteins, we have extended the experimental alanine scanning mutagenesis study to both proteins of this complex, and therefore, to all interfacial residues of this binding complex. As a result, we present new mutations, and have discovered residues important for complex formation. We have also studied the individual energy contributions for the relative binding free energy.

From alanine mutagenesis investigation obtained in numerous protein–protein interfacial residues,[41] it was expected that the functionally important residues on ZipA were those that are in direct contact with the key binding determinants of the FtsZ protein (Ile374, Phe377, and Leu378). Our main objective was attained, and we have determined some of the major FtsZ-binding determinants. Thus, we have obtained three warm spots in protein ZipA: Ile196, Lys250, and Phe269, with binding free energy differences of 2.33, 2.06, and 2.63 kcal/mol, respectively. We have also noticed the importance of residue Val194 with a free energy binding difference of 1.73 kcal/mol. These residues are in close proximity and in the middle of the hydrophobic pocket in very close contact with the warm spots present in the FtsZ peptide. We concluded also that the van der Waals interaction is the driving force for the complex binding. This fact can be rationalized by the dominant hydrophobic character of the interface, constituted mostly by direct interatomic hydrophobic contacts. The importance of the hydrophobic pocket and the vdW interactions leads to the finding that steric complementarity should probably be the determinant factor to promote the complex formation.

The warm spot of one face packs against the warm spot of its binding partner establishing a pocket region determinant for complex binding, and therefore constituting a hot spot. The hydrophobic pocket allows the burying of the interacting residues, constituting an alternative way to the O-ring formation.

The deeper knowledge of the physical nature of the protein–protein interaction surface and the definition of the binding hot spots is invaluable to drug design. These mutational data can be used to design new drugs against infectious bacterial diseases. Small molecules can be designed to bind to the residues from the warm spot cluster present in the complex between FtsZ with ZipA, hindering the complex formation, and therefore abolishing cell division. Thus, as bacterial infection is a worldwide health menace, the ZipA–FtsZ interaction is an outstanding target for antibacterial drug discovery in humans and in animals.

REFERENCES

1. Kortemme T, Baker D. Computational design of protein–protein interactions. Curr Opin Chem Biol 2004;8:91–97.
2. Russel RB, Alber F, Aloy P, Davis FP, Korkin D, Pichaud M, Topf M, Sali A. A structural perspective on protein–protein interactions. Curr Opin Struct Biol 2004;14:313–324.
3. Verkhivker GM, Bouzida D, Gehlhaar DK, Rejto PA, Freer ST, Rose PM. Computational detection of the binding-site hot spot at the remodelled human growth hormone–receptor interface. Proteins 2003;53:201–219.
4. Gao Y, Wang R, Lia L. Structure based method for analysing protein–protein interfaces. J Mol Model 2004;10:44–54.
5. Michelle RA, Mike R, DeLano WL, Hyde J, Luong TN, Oslob JD, Raphael DR, Taylor L, Wang J, McDowell RS, Wells JA, Braisted AC. Binding of small molecules to an adaptive protein–protein interface. Proc Natl Acad Sci USA 2003;100:1603–1608.
6. Pons J, Rajpal A, Kirsch J. Energetic analysis of an antigen/antibody interface: alanine scanning mutagenesis and double mutant cycles on the HyHEL-100 lysozyme interaction. Protein Sci 1999;8:958–968.
7. Keskin O, Ma B, Nussinov R. Hot regions in protein–protein interactions: the organization and contribution of structurally conserved hot spot residues. J Mol Biol 2005;345:1281–1294.
8. Halperin I, Wolfson H, Nussinov R. Protein–protein interactions; coupling of structurally conserved residues and of hot spots across interfaces. Implications for docking. Structure (Camb) 2004;12:1027–1038.
9. Hu Z, Ma B, Nussinov R. Conservation of polar residues as hot spots at protein interfaces. Proteins Struct Funct Genet 2000;39:331–342.
10. Bogan A, Thorn KS. Anatomy of hot spots in protein interfaces. J Mol Biol 1998;280:1–9.
11. Moreira IS, Fernandes PA, Ramos MJ. Computational alanine scanning mutagenesis—an improved methodological approach. Submitted.
12. Mosyak L, Zhang Y, Glasfeld E, Haney S, Stahl M, Seehra J,

Somers WS. The bacterial cell-division protein ZipA and its interaction with an FtsZ fragment revealed by X-ray crystallography. EMBO J 2000;19:3179–3191.
13. Hale CA, de Boer PA. Direct binding of FtsZ to ZipA, an essential component of the septal ring structure that mediates cell division in *E. coli*. Cell 1997;88:175–85.
14. Ohashi T, Hale CA, de Boer PA, Erickson HP. Structural evidence that the P/Q domain of ZipA is an unstructured, flexible tether between the membrane and the C-terminal FtsZ-binding domain. J Bacteriol 2002;184:4313–4315.
15. Liu Z, Mukherjee A, Lutkenhaus J. Recruitment of ZipA to the division site by interaction with FtsZ. J Mol Microbiol 1999;31: 1853–1861.
16. Wang J, Galgoci A, Kodali S, Herath KB, Jayasuriya H, Dorso K, Vicente F, Gonzalez A, Cully D, Bramhill D, Singh S. Discovery of a small molecule that inhibits cell division by blocking FtsZ, a novel therapeutic target of antibiotics. J Biol Chem 2003;45:44424–44428.
17. Jennings LD, Foreman KW, Rush TS III, Tsao DHH, Mosyak L, Li Y, Sukhdeo MN, Ding W, Dushin EG, Kenny CS, Moghazeh SL, Petersen PJ, Ruzin AV, Tuckman M, Sutherland AG. Design and synthesis of indolo[2,3-a]quinolizin-7-one inhibitors of the ZipA–FtsZ interaction. Bioorgan Med Chem Lett 2004;14:1427–1431.
18. Case DA, Darden TA, Cheatham TE III, Simmerling CL, Wang J, Duke RE, Luo R, Merz HM, Wang B, Pearlman DA, Crowley M, Brozell S, Tsui V, Gohlke H, Mongan J, Hornak V, Cui G, Beroza P, Schafmeister C, Caldwell JW, Ross WS, Kollman PA. AMBER 8. San Francisco: University of California; 2004.
19. Tsui V, Case DA. Theory and application of the Generalized Born solvation model in macromolecules simulations. Biopolymers (Nucl Acid Sci) 2001;56:275–291.
20. Cornell WD, Cieplak P, Bayly CI, Gould IR, Merz KM, Ferguson DM, Spellmeyer DC, Fox T, Caldwell JW, Kollman PA. A second generation force field for the simulation of proteins, nucleic acids, and organic molecules. J Am Chem Soc 1995;117:5179–5197.
21. Ryckaert JP, Ciccotti G, Berendsen HJ. Numerical integration of the cartesian equations of motion of a system with constraints: molecular dynamics of *n*-alkanes. J Comput Phys 1997;23:327.
22. Pastor IWR, Brooks BR, Szabo A. An analysis of the accuracy of Langevin and molecular dynamics algorithms. J Mol Phys 1998;65: 1409–1419.
23. Loncharich RJ,. Brooks BR, Pastor RW. Langevin dynamics of peptides: the frictional dependence of isomerization rates of N-actylananyl-N′-methylamide. Biopolymers 1992;32:523–535.
24. Izaguirre JA, Catarello DP, Wozniak JM, Skeel RD. Langevin stabilization of molecular dynamics. J Chem Phys 2001;114:2090–2098.
25. Huo S, Massova I, Kollman PA. Computational alanine scanning of the 1:1 human growth hormone–receptor complex. J Comput Chem 2002;23:15–27.
26. Rocchia W, Sridharan S, Nicholls A, Alexov E, Chiabrera A, Honig B. Rapid grid-based construction of the molecular surface for both molecules and geometric objects: applications to the finite difference Poisson-Boltzmann method. J Comp Chem 2002;23:128–137.
27. Rocchia W, Alexov E, Honig B. Extending the applicability of the nonlinear Poisson-Boltzmann equation: multiple dielectric constants and multivalent ions. J Phys Chem B 2001;105:6507–6514.
28. Moreira IS, Fernandes PA, Ramos MJ. Accuracy of the numerical differentiation of the Poisson-Boltzmann equation. J Mol Struct. (Theochem) 2005;729:11–18.
29. Connolly ML. Analytical molecular surface calculation. J Appl Crystallogr 1983;16:548–558.
30. Kollman PA, Massova I, Reyes C, Kuhn B, Huo S, Chong L, Lee M, Lee T, Duan Y, Wang W, Donini O, Cieplak P, Srinivasan J, Case DA, Cheatham TE III. Calculating structures and free energies of complex molecules: combining molecular mechanics and continuum models. Acc Chem Res 2000;33:889–897.
31. Wang W, Donini O, Reyes CM, Kollman PA. Biomolecular simulations: recent developments in force field, simulations of enzyme catalysis, protein–ligand, protein–protein, and protein–nucleic acid noncovalent interactions. A Rev Biophys Biomol Struct 2001;30:211–243.
32. Massova I, Kollman PA. Computational alanine scanning to probe protein–protein interactions: a novel approach to evaluate binding free energies. J Am Chem Soc 1999;121:8133–8143.
33. Wang J, Morin P, Wang W, kollman PA. Use of MM-PBSA in reproducing the binding free energies to HIV-1 RT of TIBO derivatives and predicting the binding mode to HIV-1 RT of efavirenz by docking and MM-PBSA. J Am Chem Soc. 2001;123: 5221–5230.
34. Wang W, Kollman PA. Free energy calculations on dimer stability of the HIV protease using molecular dynamics and a continuum solvent model. J Mol Biol 2000;303:567–582.
35. Reyes CM, Kollman PA. Investigating the binding specificity of U1A-RNA by computational mutagenesis. J Mol Biol 2002;295: 1–6.
36. Cohlke H, Case DA. Converging free energy estimates: MM-PB(GB)SA studies on the protein–protein complex Ras-Raf. J Comput Chem 2004;25:238–250.
37. Xia B, Tsui V, Case DA, Dyson J, Wright PE. Comparison of protein solution structures refined by molecular dynamics simulations in vacuum, with a generalized Born model, and with explicit water. J Biomol NMR 2002;22:317–331.
38. Kuntz ID, Chen K, Sharp KA, Kollman PA. The maximal affinity of ligands. Proc Natl Acad Sci 1999;96:9997.
39. Sheinerman FB, Norel R, Honig B. Electrostatics aspects of protein-protein interactions. Curr Opin Struct Biol 2002;10:153–159.
40. Kumar S, Nussinov R. Close-range electrostatic interactions in proteins. Chembiochem 2002;3:604–617.
41. Clackson T, Wells JA. A hot-spot of binding energy in a hormone–receptor interface. Science 1995;267:383–386.